JOC Article

Structure−Property Relationships in Conjugated Donor−Acceptor Molecules Based on Cyanoanthracene: Computational and Experimental Studies

Jui-Hsien Lin, Arumugasamy Elangovan,† and Tong-Ing Ho*

Department of Chemistry, National Taiwan University, Taipei - 106, Taiwan

hall@ntu.edu.tw

Received June 11, 2005

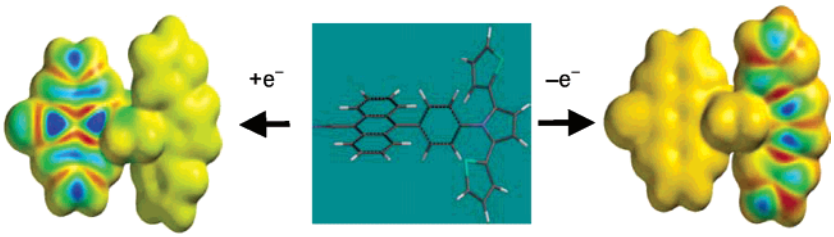

Two series of π-conjugated bipolar compounds, namely, 9-phenyl-10-anthronitriles (**PAN** series) and 9-phenylethynyl-10-anthronitriles (**PEAN** series), having inherent redox centers have been synthesized and their electronic absorption, fluorescence emission, and electrochemical behavior have been studied. Electrochemiluminescence of these molecules bearing weak, strong, and spin-polarized donors is also studied. The observed electronic properties are explained with the help of results obtained from density functional theory (DFT- B3LYP/6-31G*) calculations. The structure−property relationships of all the molecules are discussed.

Introduction

Organic π-conjugated donor−acceptor (D−A) molecular materials have attracted significant attention due to their potential application in electronics such as electrooptic devices,[1] light-emitting diodes,[2] and field effect transistors.[3] The synthetic ability of organic chemists coupled with the wealth of fabrication techniques available to materials scientists and engineers contribute to the realization of materials for our future needs. Suzuki coupling and Sonogashira coupling approaches have proved to be some of the best established techniques for the synthesis of a wide variety of conjugated organic materials.[4]

Charge recombination of electrolytically generated radical ions in solutions leads to the formation of electronically excited states of molecules by energetic electron-transfer reactions at the electrified interface. Such excited species emit energy in the form of fluorescence of a certain wavelength. This process is called electrogenerated chemiluminescence or electrochemiluminescence (ECL).[5] ECL emission is believed to occur via one of the three different routes: directly from singlet excited state (S-route), via triplet−triplet annihilation (T-route), or via excimer formation (E-route).[6] Excimers are homodimers that exist in the photoexcited state of molecules in solution.[7] Many excimers are formed between molecules whose π-systems interact effectively, leading to the formation of appropriate states, and they possess structures prominently governed by their monomer chemical structures. The formation of excited states in the solid state by the application of an electric field

† Present address: Department of Chemistry, University of Washington, Seattle, WA 98195.

* Fax: +886-2-23636359.

(1) (a) Shi, Y.; Zhang, C.; Zhang, H.; Bechtel, J. H.; Dalton, L. R.; Robinson, B. H.; Steier, W. H. *Science* **2000**, *288*, 119. (b) Dalton, L. R.; Steier, W. H.; Robinson, B. H.; Zhang, C.; Ren, A.; Garner, S.; Chen, A.; Londergan, T.; Irwin, L.; Carlson, B.; Fifield, L.; Phelan, G.; Kincaid, C.; Amend, J.; Jen, A. *J. Mater. Chem.* **1999**, *9*, 1905.

(2) (a) Friend, R. H.; Gymer, R. W.; Holmes, A. B.; Burroughes, J. H.; Marks, R. N.; Taliani, C.; Bradley, D. D. C.; Dos Santos, D. A.; Brédas, J.-L.; Lögdlund M.; Salaneck, W. R. *Nature* **1999**, *397*, 121. (b) Kraft, A.; Grimsdale A. C.; Holmes, A. B. *Angew. Chem., Int. Ed.* **1998**, *37*, 402.

(3) Brown, A. R.; Pomp, A.; Hart C. M.; de Leeuw, D. M. *Science* **1995**, *270*, 972.

(4) (a) Wonag, K.-T.; Hung, T. S.; Lin, Y.; Wu, C.-C.; Lee, G.-H.; Peng, S.-M.; Chou, C.-H.; Su, O. Y. *Org. Lett.* **2002**, *4*, 513. (b) Yamaguchi, Y.; Kobayashi, S.; Miyamura, S.; Okamoto, Y.; Wakamiya, T.; Matsubura, Y.; Yoshida, Z.-i. *Angew. Chem., Int. Ed.* **2004**, *43*, 366. (c) Boydston, A. J.; Yin, Y.; Pagenkopf, B. L. *J. Am. Chem. Soc.* **2004**, *126*, 3724. (d) Odom, S. A.; Parkin, S. R.; Anthony, J. E. *Org. Lett.* **2003**, *5*, 4245, (e) Pohl, R.; Anzenbacher, P., Jr. *Org. Lett.* **2003**, *5*, 2769. (f) Metivier, R.; Amengual, R.; Leray, I.; Michelet, V.; Genet, J.-P. *Org. Lett.* **2004**, *6*, 739.

10.1021/jo051183g CCC: $30.25
Published on Web 08/05/2005

(as in OLEDs) has been shown to follow a mechanism similar to that in solution (ECL).[8] Hence, the study of electronic properties of more new donor−acceptor molecular systems is necessary to gain a better understanding of the basis underlying the electron-transfer processes occurring in the materials upon interaction with external stimuli such as electromagnetic radiation and addition and removal of electrons to and from the molecules.

In the present work, two series of compounds, namely, biaryls (9-phenyl-10-anthronitriles, **PANs**) and biarylethynes (9-phenylethynyl-10-anthronitriles, **PEANs**), having donor−acceptor character were synthesized and their photophysical properties, electrochemical characteristics, and ECL were studied. The donors are methoxy- (ie., anisole, **An**-), *p*-*N*,*N*-(dimethylamino)- (**DMA**-), *p*-(2,5-dithienyl)pyrrolyl- (**DTP**-), and *N*,*N*-di-*p*-anisylamino- (**An$_2$*N*-**) substituted phenyls, and the acceptor is the anthronitrile (**AN**) moiety. The approach is to provide the fluorophore **AN** with incremental electron-donating strength at the phenyl moiety from no donor to weak (OMe) to strong (NMe_2) donors and high-spin donors [*N*-(2,5-dithienylpyrrolyl)phenyl- (**DTP-P**) and *N*,*N*-di-*p*-anisylaminophenyl- (**An$_2$***N*-P)] in both series (the ethynyl linkage is denoted by **E**).

The triarylamino and the dithienylpyrrolyl (high-spin) donors have been chosen in view of the substantial amount of research done on them by Sugawara,[9a] Jen[9b] Yano,[10] Blackstock,[11] and Lambert[12] on the synthesis and study of adiabatic electron-transfer properties in certain mixed-valence systems.

The anthronitrile (**AN**) moiety has been chosen in view of the fact that it is an excellent fluorophore and a strong electron acceptor. Moreover, 9-cyano-10-halo anthracenes have been found to afford, upon electroreduction, radical anion intermediates stable enough for the electrochemical studies.[13] Substitution of the halogen with electron-donating groups via conjugation would help achieve new materials having tunable properties. The anthronitrile moiety can additionally impart intermolecular $\pi-\pi$ interaction, and by appropriate choice of conditions, the chromophore activity can be controlled and the emission can be tuned.

Results and Discussion

The chemical structures of the compounds studied in the present work are listed in Chart 1. Compounds of the **PAN** series were synthesized by palladium-catalyzed Suzuki coupling[14] of 9-bromo-10-cyanoanthracene (**Br-AN**) with the corresponding donor-substituted phenylboronic acids. The **PEAN** series of internal ethynes were prepared by the coupling reaction of the corresponding terminal aryl acetylenes with **Br-AN** under modified Sonogashira conditions.[15] A summary of the photophysical data of these compounds is presented in Table 1, and their electrochemical characteristics are furnished in Table 2.

Photophysical Properties

The photophysical characteristics of the two series of compounds are given in Table 1. The UV−vis absorption spectra of all the compounds recorded in CH_2Cl_2 showed an absorption at about 270 nm characteristic (β-band) of an anthracene unit. The $\pi-\pi^*$ transition region of electronic absorption spectra is shown in Figure 1. Figure 1a depicts the electronic absorption spectra of the **PAN** series in which one can see the pronounced effect of structural modification. While all molecules show structured $\pi-\pi^*$ that can be attributed to the local excitation (LE) all centered around 410 nm, **DMA-PAN** and **An$_2$*N*-PAN** show a moderate charge transfer component as seen from the appearance of a shoulderlike hump around 420 nm accompanied by some degree of loss of fine structure. Surprisingly, the **DTP-PAN** (though bearing an electron-donating **DTP**-) did not exhibit a similar trend; instead, while retaining the major part of its vibrational fine structure along the lines of **PAN** and **AnAN** in its absorption, it shows an unusual band around 350 nm. One explanation could be that this band might arise from the probability of an intramoiety charge transfer from the pyrrole (donor) moiety to the thiophenyl (acceptor) moiety. The effect of extension of π-conjugation is evident from the absorption spectra of the **PEAN** series. It can be seen from Figure 1b that, for those **PEANs** having poor donors (**PEAN** and **AnEAN**), the longest wavelength of absorption maximum falls at about 440 nm as structured bands at a wavelength that is red-shifted by about 40 nm as compared with the **PAN** series. The vertically excited lowest singlet state (the Franck−Condon state) experiences no charge transfer as in **PAN**

(5) (a) Faulkner, L. R.; Bard, A. J. Electrogenerated Chemiluminescence. In *Electrochemical Methods*; John Wiley & Sons: New York, 1980; pp 621−627. (b) Faulkner L. R.; Bard, A. J. In *Electroanalytical Chemistry;* Bard, A. J., Ed.; Marcel Dekker: New York, 1977; Vol. 10, pp 1−95. (c) Knight, A. W.; Greenway, G. M. *Analyst* **1994**, *119*, 879. (d) Knight, A. W. *Trends Anal. Chem.* **1999**, *18*, 47. (e) Richter, M. M. *Chem. Rev.* **2004**, *104*, 3003. (f) Lai, R. Y.; Fabrizio, E. F.; Jenekhe, S. A.; Bard, A. J. *J. Am. Chem. Soc.* **2001**, *123*, 9112. (g) Knorr, A.; Daub, J. *Angew. Chem., Int. Ed.* **1995**, *34*, 2664. (h) Prieto, I.; Teetsov, J.; Fox, M. A.; Vanden Bout, D. A.; Bard, A. J. *J. Phys. Chem*. **2001**, *A105*, 520. (i) Oyama, M.; Okazaki, S. *Anal. Chem*. **1998**, *70*, 5079. (j) Kapturkievicz, A. *J. Electroanal. Chem*. **1990**, *290*, 135. (k) Kapturkievicz, A. *J. Electroanal. Chem*. **1991**, *302*, 13. (l) Faulkner, L. R.; Tachikawa, H.; Bard, A. J. *J. Am. Chem. Soc*. **1972**, *94*, 691.

(6) Faulkner, L. R.; Bard, A. J. In *Electroanalytical Chemistry*; Bard, A. J., Ed.; Marcel Dekker: New York, 1977; Vol. 10, pp 1−95.

(7) Turro, N. J. *Modern Molecular Photochemistry*; The Benjamin/Cummings Publishing Co., Inc.: Menlo Park, CA, 1978.

(8) (a) Anderson, J. D.; et al. *J. Am. Chem. Soc.* **1998**, *120*, 9646. (b) Armstrong, N. R.; Anderson, J. D.; Lee, P. A.; McDonald, E. M.; Wightman, R. M.; Hall, H. K.; Hopkins, T.; Padias, A.; Thayumanavan, S.; Barlow, S.; Marder, S. R. *SPIE* **1999**, *3476*, 178. (c) Armstrong, N. R.; Whightman, R. M.; Gross, E. M. *Annu. Rev. Phys. Chem*. **2001**, *52*, 391.

(9) (a) Nakazaki, J.; Chung, I.; Matsushita, M. M.; Sugawara, T.; Watanabe, R.; Izuoka, A.; Kawada, Y. *J. Mater. Chem*. **2003**, *13*, 1011. (b) Kim, K.-S.; Kang, M.-S.; Ma. H.; Jen, A. K.-Y. *Chem. Mater*. **2004**, *16*, 1558.

(10) (a) Sato, K.; Yano, M.; Furuichi, M.; Shiomi, D.; Abe, K.; Takui, T.; Itoh, K.; Higuchi, A.; Katuma, K.; Shirota, Y. *J. Am. Chem. Soc*. **1997**, *119*, 6607. (b) Yano, M.; Ishida, Y.; Aoyama, K.; Tatsumi, M.; Sato, K.; Shiomi, D.; Ichimura, A.; Takui, T. *Synth. Metals* **2003**, *137*, 1275.

(11) (a) Stickley, K. R.; Blackstock, S. C. *J. Am. Chem. Soc*. **1994**, *116*, 11576. (b) Stickley, K. R.; Selby, T. D.; Blackstock, A. C. *J. Org. Chem*. **1997**, *62*, 448.

(12) (a) Lambert, C.; Nöll, G.; Schelter, J. *Nat. Mater.* **2002**, *1*, 69. (b) Lambert, C.; Nöll, G.; Schmälzlin, E.; Meerholz, K.; Bräuchele, C. *Chem. Eur. J*. **1998**, *4*, 2129. (c) Heckmann, A.; Lambert, C.; Goebel, M.; Wortmann, R. *Angew. Chem*., *Int. Ed*. **2004**, *43*, 5851. (d) Lambert, C.; Nöll, G. *J. Am. Chem. Soc*. **1999**, *121*, 8434. (e) Lambert, C.; Nöll, G. *J. Chem. Soc., Perkin Trans. 2* **2002**, 2039.

(13) Heinze, J.; Schwart, J. *J. Electroanal. Chem*. **1981**, *126*, 283.

(14) Miyaura, N.; Suzuki, A. *Chem. Rev.* **1995**, *95*, 2457.

(15) (a) Elangovan, A.; Wang, Y.-H.; Ho, T.-I. *Org. Lett*. **2003**, *5*, 1841. (b) Sonogashira, K.; Tohda, Y.; Hagihara, N. *Tetrahedron Lett*. **1975**, *16*, 4467.

CHART 1. Chemical Structures of Compounds Studied in the Present Work: PAN Series (Top) and PEAN Series (Bottom)

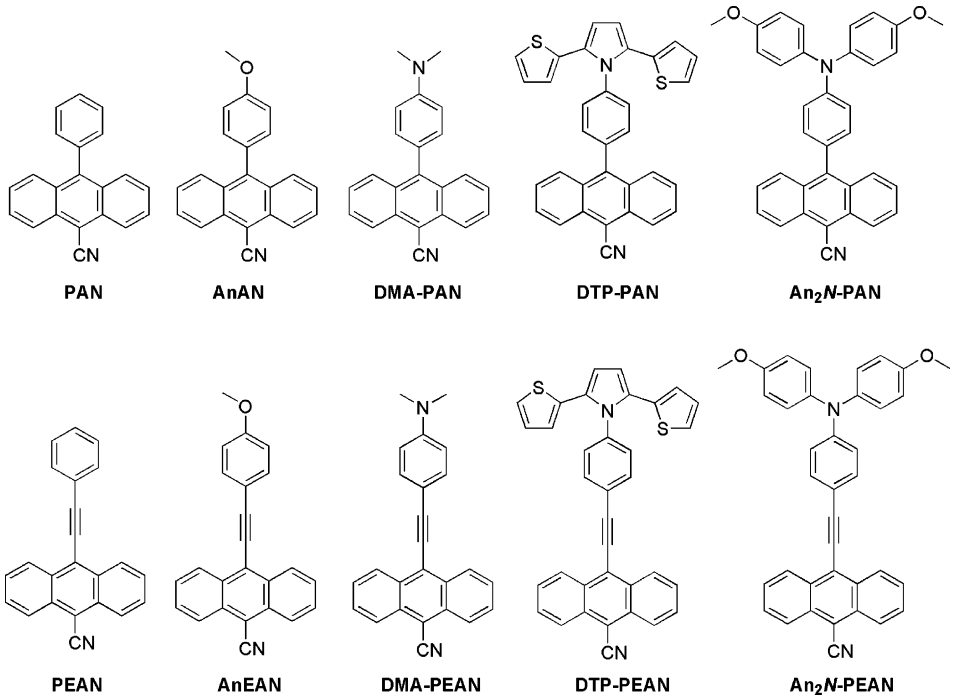

TABLE 1. Photophysical Data of PANs and PEANs

compounds	λ_{max}^{abs} (nm)	ΔE_{HL} (eV)[a]	ϵ_{max}[b]	λ_{max}^{flu} (nm)	Φ[c]
PAN	389	2.85	0.68	455	0.46
AnAN	390	2.85	0.84	470	0.10
DMA-PAN	408	2.48	0.44	562	0.09
DTP-PAN	388	2.85	0.42	443	0.004
An$_2$*N*-PAN	410	2.48	0.80	454	0.03
PEAN	422	2.64	1.46	465	0.86
AnPEAN	430	2.64	1.74	485	0.71
DMA-PEAN	483	2.25	3.07	588	0.04
DTP-PEAN	424	2.64	2.50	469	0.001
An$_2$*N*-PEAN	490	2.25	3.38	574	0.002

[a] ΔE_{HL}: HOMO−LUMO gap calculated from the onset of the visible absorption maxima. [b] ($\times 10^4$ M^{-1} cm^{-1}). [c] Using coumarin 334 standard (Φ 0.69 in MeOH).[16]

and **AnAN**. For the **PEAN** having a stronger donor (**DMA-PEAN** and **An$_2$*N*-PEAN**), the absorption shifts to >483 nm with a structureless feature. This vast red shift can be attributed to absorption due to charge-transfer transition at the lowest Franck−Condon excited state. In this series also the **DTP**-substituted molecule **DTP-PEAN** behaves similar to **DTP-PAN** in that the LE band is retained with the appearance of an additional band around 300−350 nm.

The fluorescence spectra of the **PAN** series (Figure 2a) and **PEAN** series (Figure 2b) are interesting to study. **PAN** and **An$_2$*N*-PAN** show surprisingly similar emission patterns, while **DMA-PAN** alone shows a charge-transfer spectrum. While all compounds in the **PAN** series show emission maxima close to 440 nm (the so-called **B** band), compounds **DMA-PAN** and **DTP-PAN** show additional, more intense **A** bands at 570 and 520 nm respectively. This observation of dual fluorescence in these two systems may be attributable to the existence of twisted intramolecular charge transfer states (TICTs).[17] It may be noted that this kind of dual fluorescence (vis-à-vis TICT state) is absent when the donor and acceptor are separated by an ethynyl π-bridge. In fact, the **DTP-PEAN** shows emission similar to that of **PEAN**. The **AnAN** shows moderate charge transfer, but this does not seem to effect a major shift in the emission wavelength as compared with **DMA-PAN**. In Figure 2b, compounds **PEAN** and **DTP-PEAN** emit closely at the same maxima with vibrational fine structure, while **AnEAN** attains moderate charge-transfer character given its structureless emission band again due to the subtle increase in donor strength replacing H with OMe (Figure 2b). Compounds **DMA-PEAN** and **An$_2$*N*-PEAN** show vast red-shifted fluorescence emission at 590 and 575 nm, respectively, which can be assigned to an excited-state charge-transfer transition.

On comparison of the data in Table 1, the **PEAN** series shows absorption red-shifted by 30−90 nm as compared with the **PAN** series. Similarly, the fluorescence spectra show a 10−125 nm red shift as compared with **PAN** series. Thus, extension of π-conjugation shifted the electronic properties in the desirable region useful for light-emitting applications. In general, the **PEAN** series has been found to show absorption and emission substantially red-shifted (into the visible region) as compared with **PANs** and free **AN** ($\lambda_{max}^{abs} = 400$ nm; $\lambda_{max}^{flu} = 440$).

(16) Reynolds G. A.; Drexhage, K. H. *Optics Commun*. **1975**, *13*, 222.
(17) (a) Rettig, W. Electron-Transfer I. In *Topics in Current Chemistry*; Mattay, J., Ed..; Springer-Verlag: Berlin, 1994; Chapter 5, p 253. (b) Rotkiewicz, K.; Grellmann, K. H.; Grabowski, Z. R. *Chem. Phys. Lett.* **1973**, *19*, 315. (c) Grabowski, Z. R.; Rotkiewicz, K.; Siemiarczuk, A.; Cowley, D. J.; Baumann, W. *Nouv. J. Chim.* **1979**, *3*, 443. (d) Rettig, W. *Angew. Chem., Int. Ed. Engl.* **1986**, *25*, 971. (e) Rettig, W.; Maus, M. In *Conformational Analysis of Molecules in Excited States*; Waluk, J., Ed.; Wiley-VCH: New York, 2000; Chapter 1, pp 1−55. (f) Grabowski, Z. R.; Rotkiewicz, K. *Chem. Rev*. **2003**, *103*, 3899. (g) Yang, J.-S.; Liau, K.-L.; Wang, C.-M.; Hwang, C.-Y. *J. Am. Chem. Soc.* **2004**, *126*, 12325. (h) Klock, A. M.; Rettig, W. *Polish J. Chem*. **1993**, *67*, 1375. (i) Baumann, W.; Schwager, B.; Detzer, N.; Okada, T.; Mataga, N. *Bull. Chem. Soc. Jpn*. **1987**, *60*, 4245.

TABLE 2. ECL and Electrochemical Data for PANs and PEANs Recorded in Acetonitrile and Dichloromethane with 50 mM TBAP at a Scan Rate of 50 mV/s

			$E_{p,ox}$ (V)		$E_{p,red}$ (V)		ΔE_{HL} (eV)[a]		$-\Delta H°$ (eV)[b]	
compound	λ_{max}^{ECL} (nm, eV)		MeCN	CH_2Cl_2	MeCN	CH_2Cl_2	MeCN	CH_2Cl_2	MeCN	CH_2Cl_2
PAN	456	2.72	1.79	1.80	−1.13	−1.55	2.92	3.35	2.76	3.19
AnAN	480	2.58	1.71	1.48	−1.32	−1.53	3.23	3.01	2.87	2.85
DMA-PAN	538	2.30	1.68	1.08	−1.09	−1.58	2.77	2.66	2.61	2.50
DTP-PAN	535	2.32	0.89	0.86	−1.28	−1.56	2.17	2.42	2.01	2.26
An_2N-PAN	512	2.42	0.86	0.86	−1.36	−1.37	2.22	2.43	2.06	2.07
PEAN	552	2.25	1.62	1.14	−0.92	−1.24	2.54	2.38	2.38	2.22
AnPEAN	547	2.27	1.49	0.82	−0.89	−1.32	2.38	2.14	2.22	1.98
DMA-PEAN	588	2.11	0.90	0.97	−0.90	−1.35	1.80	2.32	1.64	2.16
DTP-PEAN	590	2.10	0.96	0.87	−1.00	−1.30	1.96	2.17	1.80	2.01
An_2N-PEAN		2.72	1.00	0.90	−1.05	−1.29	2.05	2.19	1.89	2.03

[a] HOMO−LUMO gap calculated as the difference between the two peak potentials. [b] Calculated using the equation $\Delta H° = E_{p,ox} - E_{p,red} - 0.16$.[5k]

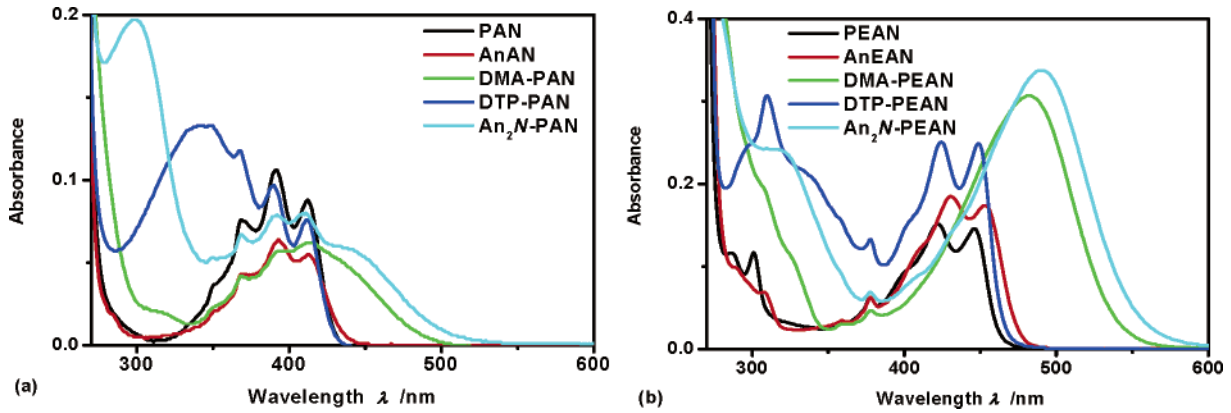

FIGURE 1. UV−visible absorption spectra of **PAN** series (a) and **PEAN** series (b) in CH_2Cl_2 (10^{-5} M).

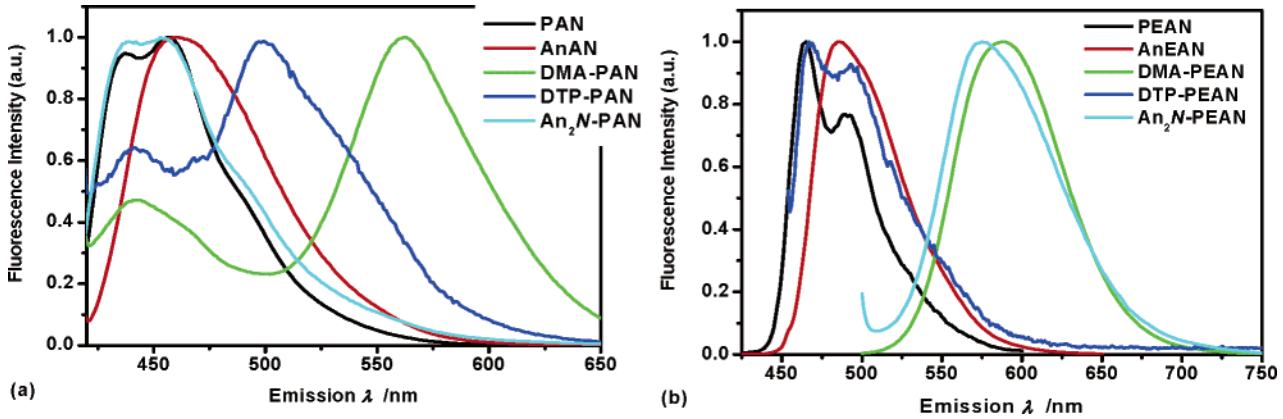

FIGURE 2. Fluorescence emission spectra of **PANs** (a) and **PEANs** (b) in CH_2Cl_2 (10^{-5} M).

The photoluminescence quantum yields (Φ measured in CH_2Cl_2) are moderate to quite high for the **PEAN** series as compared with the **PAN** series, especially the weak donor-substituted ones (Table 1). In both series, weak donor-substituted compounds show higher Φ than strong donor-substituted compounds. The optical band gap (ΔE_{HL}) calculated from the onset of the absorption maxima are found to be in the exploitable region for emitting devices. The ΔE_{HL} has been decreased to near 2.25 eV for ethynes as compared with directly linked biaryls for which it remains between 2.48 and 2.9 eV. These properties arise due to the donor−acceptor character of these molecules and extension of π-conjugation particularly in **PEAN** series.

The existence of ICT character can be understood very well by testing the ability of the solute molecules in undergoing shifts in their emission maxima with increasing solvent polarity. Hence, the solvatochromic spectra of these fluorophore materials were checked by choosing different solvents of varying polarity ranging from nonpolar hexane through highly polar DMSO. The solvatochromic fluorescence spectra of all compounds are provided in Figure 3. It is interesting to note that the general solvatochromic trend in both the series is almost identical; however, a case by case analysis is worthwhile. Neither **PAN** nor **PEAN** experienced any solute−solvent dipole−dielectric interaction as seen from the absence of ICT fluorescence bands, though there is a very mild red

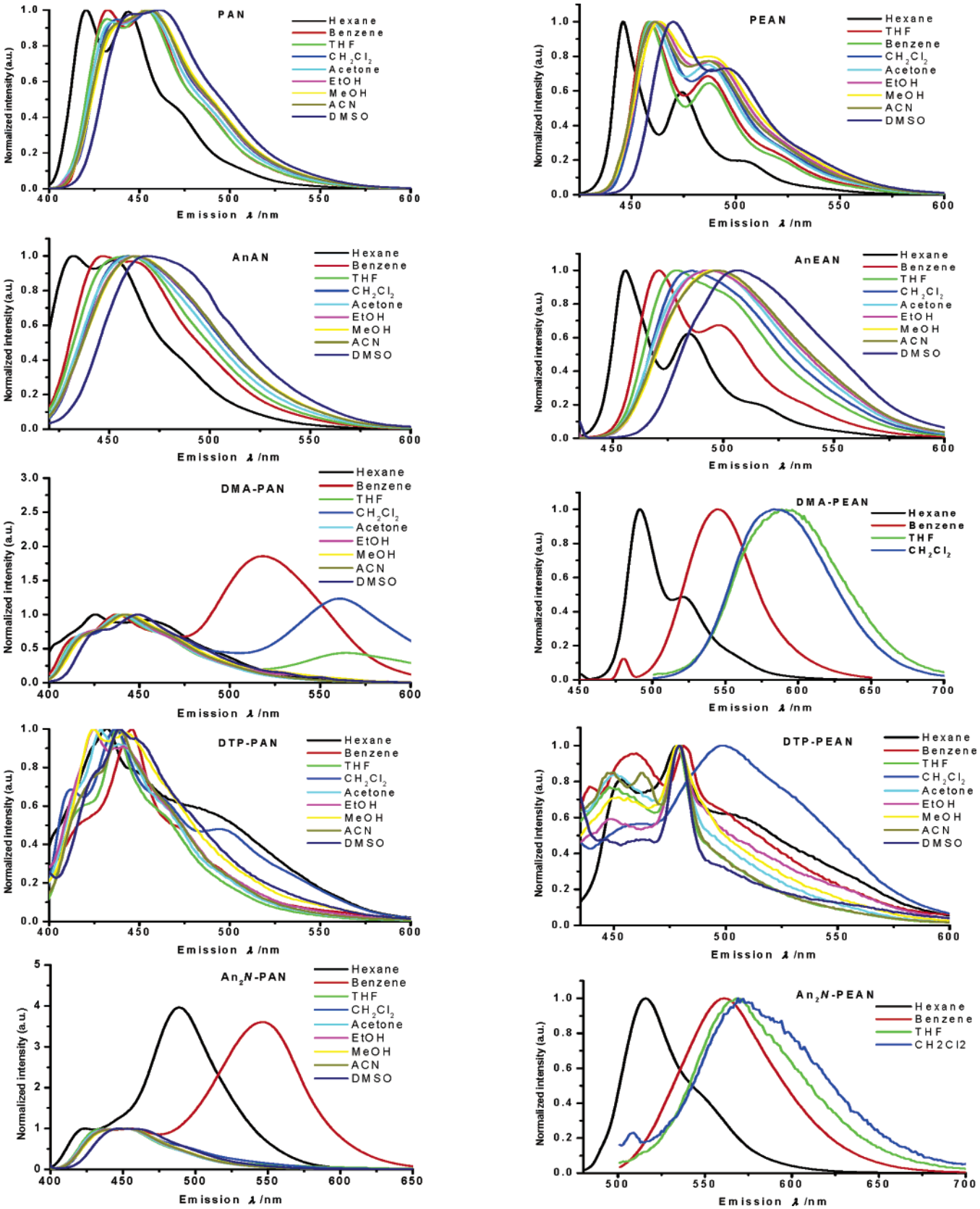

FIGURE 3. Fluorescence solvatochromic spectra of **PANs** (left column) and **PEANs** (right column) recorded in various solvents of differing polarity. **DMA-PEAN** and **An$_2$*N*-PEAN** are not fluorescent in solvents higher in polarity than CH_2Cl_2.

shift in the emission maxima. Upon substitution of a moderately strong donor, OMe group, the maxima gradually loose their vibronic structure and attain a structureless feature when going from less polar hexane through

more polar DMSO. The effect of ethyne substitution is well pronounced in the case of **AnEAN** as compared with **AnAN** in that the red shift is more noticeable and well resolved in the spectra of the former in comparison to that of the latter.

Amino-substituted **DMA-PAN** and **An$_2$*N*-PAN** show two different emission maxima. The first emission band is centered around 450 nm with fine structures for both molecules. This band can be described as LE emission and does not appear to be affected by the solvent dielectric constant. The second, structured A band, which is more intense than the structureless B band appearing at a longer wavelength (>520 nm) and is likely due to the TICT state, alone undergoes a shift to the much lower energy region with increasing solvent polarity and with concomitant reduction in the intensity. This kind of TICT is not observed in the case of ethynyl counterparts of these two chromophores, namely, the **DMA-PEAN** and **An$_2$*N*-PEAN**. This could be due to the fact that the ethynyl bridge allows for conformational twisting with respect to its long axis, and as a result, ICT in the twisted state is not possible and only normal ICT is observed. The absence of dual-fluorescence in **PEANs** confirms that the observation of A bands in **DMA-PAN** and **An$_2$*N*-PAN** is due to the TICT transition. The ICT in the ethyne-linked donor acceptor molecules is more noticeable, as stated above, than in directly linked **PANs** with a larger red shift (>100 nm) going from hexane to CH_2Cl_2. An additional interesting point is the failure to observe any influence of solvent polarity on the emission behavior of dithienylpyrrole-substituted **PAN** and **PEAN**. Both **DTP-PAN** and **DTP-PEAN** show similar patterns of spectra in the solvatochromic studies in that there is no pronounced shift in the emission maximum upon increasing the dielectric constant of the media, though only CH_2Cl_2 causes a shift in the emission of **DTP-PEAN** (500 nm band), and this could be from an excimer state as also noticed in the case of **DTP-PAN**.

A fluorophore, by the virtue of its electronic structure, is considered to be a dipole. This dipole (with a dipole moment μ) in solution can interact with its surroundings, the medium characterized by its dielectric constant (ϵ) and refractive index (n). This interaction produces changes in energy of both the ground state and excited state of the molecule. As a result, the fluorophore emits light of different energies, and the difference between the ground state and excited-state energy levels is given as the Stokes shift. This Stokes shift is a property of the solvent refractive index and dielectric constant. The influence of the local molecular environment on the optical property of the molecules studied here can be understood by using the Lippert equation; a model that describes the interactions between the solvent and the dipole moment of chromophore.[18]

$$\nu_{abs} - \nu_{flu} = 2/hc[\Delta f]\{(\mu^* - \mu)^2/a^3\} + \text{Constant}$$

where

$$\Delta f = [(\epsilon - 1)/(2\epsilon + 1)] - [(n^2 - 1)/(2n^2 + 1)]$$

and a is the radius of the chromophore

A plot of the polarity (or the orientation polarizability, Δf) of the solvents against the Stokes shift for selected compounds in various solvents is shown in Figure 4. The observed linear correlation between the Stokes shift and the Δf illustrates the adherence of experimental data to the Lippert equation in the case of **AnEAN**. Other molecules show moderate deviation reflecting the observation of regular (and irregular) red shift in the emission maxima (see Figure 3).

Electrochemistry. To determine the electrochemical activity and to arrive at the reduction and oxidation potential values of these compounds, cyclic voltammograms (CV) were recorded. CV of **PANs** and **PEANs** (1.0×10^{-3} M) were recorded in acetonitrile as well as in CH_2Cl_2 with 50 mM tetrabutylammonium perchlorate (TBAP) as a supporting electrolyte at a scan rate of 0.05 V/s, and the reduction and oxidation peak potentials are shown in Table 2.

The scan rates were varied from 50 to 125 mV in increments of 25 mV in an attempt to see any variation in the peak potential with change in scan rates. Figure 5 shows CV curves recorded for **An$_2$*N*-PAN** and **An$_2$*N*-PEAN**, and, as expected, these compounds showed reversible oxidation and reversible reduction one-electron transfer reactions. No significant shift in the peak potentials was observed with varying scan rates, and only the current was found to be reduced. Among the two series of compounds, **PANs** showed moderate to very good electrochemical reversibility (see Supporting Information for values) in both oxidation and reduction cycles; in contrast, **PEANs** (except **DTP-PEAN** and **An$_2$*N*-PEAN**) showed irreversible oxidation in both MeCN and CH_2Cl_2, although unsubstituted **PEAN** showed moderate reversibility of oxidation reaction in CH_2Cl_2 but complete irreversibility in MeCN.

In less polar CH_2Cl_2, the reversible reduction peak potentials, which correspond to the reduction at the 9-cyanoanthracene moiety, occur in the vicinity of around -1.3 V for **PEANs**, whereas they occur at about -1.55 V for **PANs**. The extension of conjugation via a C$-$C triple bond has altered the reduction potential favorably.

Computation

The observation of the electronic properties can be better understood by analyzing the results obtained from density functional calculations carried out using Becke's three parameter set with Lee$-$Yang$-$Parr modification (B3LYP) with the 6-31G* basis set of theory.[19] The calculated highest occupied molecular orbital (HOMO) and the lowest unoccupied molecular orbital (LUMO) surfaces of the molecules **PAN** and **AnAN** both have twisted structures in the energy-minimized gas-phase geometry. Their HOMO and LUMO are both localized on the acceptor AN moiety. All electronic properties are hence governed by these orbitals, and, as a result, we observe structured absorption and LE emission for these two molecules. For **DMA-PAN** and **An$_2$*N*-PAN**, the HOMO is localized in the donor site (NMe_2 and An_2N-)

(18) (a) Lakovickz, J. R. *Principles of Fluorescence Spectroscopy* Plenum Press: New York, 1983; p 187 (b) Lippert, Von E. *Z. Electrochem.* **1957**, *61*, 962.

(19) (a) Lee, C.; Yang, W.; Parr, R. G. *Phys. Rev. B* **1988**, *37*, 785. (b) Beck, A. D. *J. Chem. Phys.* **1993**, *98*, 5648.

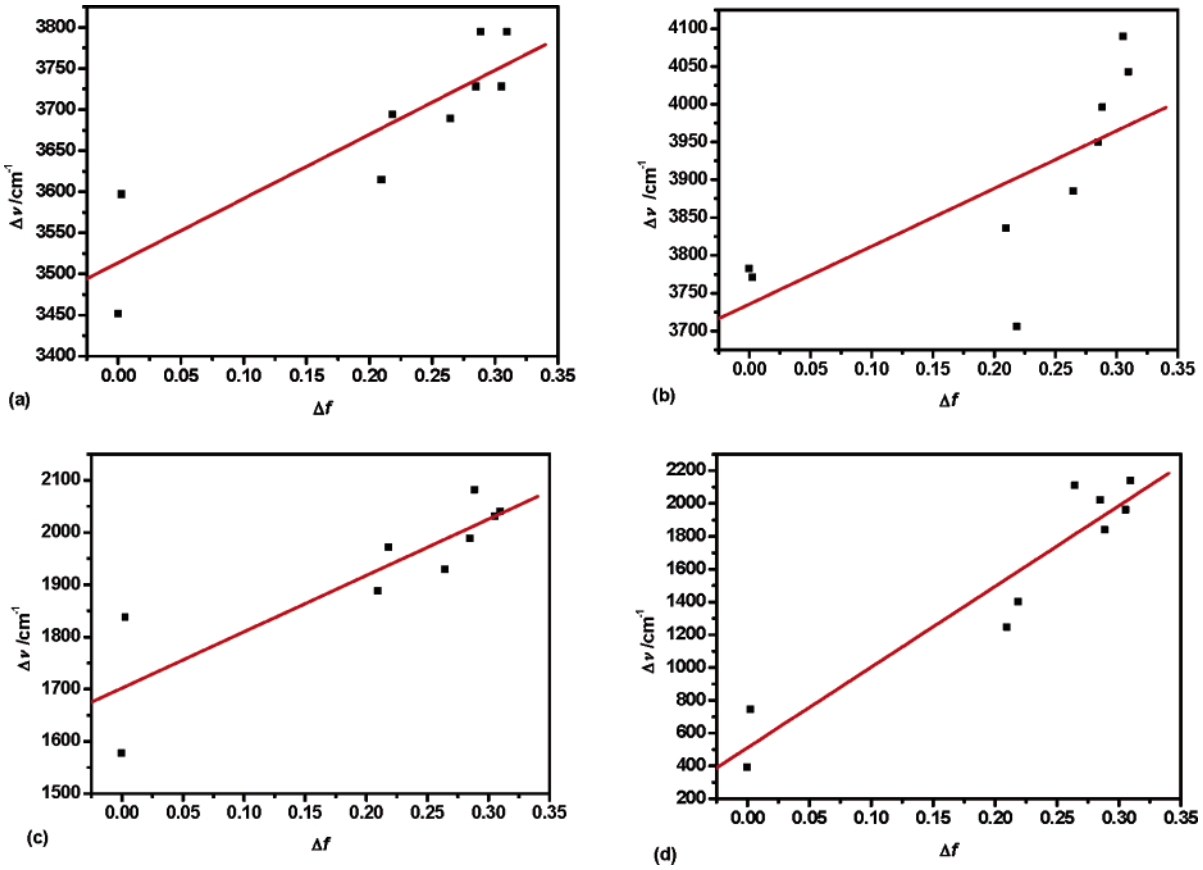

FIGURE 4. Linear correlation of orientation polarization (Δf) of solvent media with Stokes shift ($\Delta \nu$) for **PAN** (a), **AnAN** (b), **PEAN** (c), and **AnEAN** (d). See Supporting Information for data tables of all compounds.

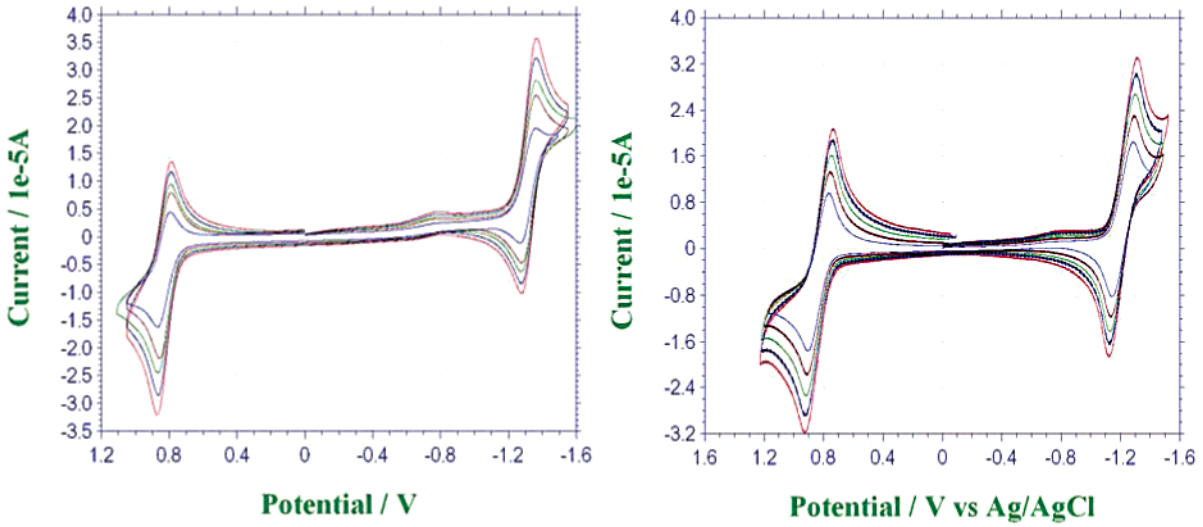

FIGURE 5. CV traces of **An$_2$*N*-PAN** (left) and **An$_2$*N*-PEAN** (right) recorded with reference to Ag/Ag$^+$ at different scan rates in CH_2Cl_2 (10^{-3} M with 50 mM TBAP). Color code: red, 50 mV; blue, 75 mV; green, 100 mV; crimson, 125 mV; navy blue, 150 mV.

groups with some degree of orbital coefficients on the phenylene bridge, whereas the LUMO is located mainly on the acceptor AN moiety. Therefore, probable intramolecular charge transfer (ICT) transition can be expected in these two systems. Considering **DTP-PAN**, there seems to be no involvement of phenylene bridge, and there is no adequate contribution to either the HOMO or the LUMO. Thus, the donor π-electron remains cut off from the LUMO coefficients, and hence there can be no communication between the two parts. This is evident from the observation of absorption and emission spectra that do not reveal any ICT character for this particular compound.

The same trend can be observed for the **PEAN** series (Figure 7). The poor-donor-substituted **PEAN**, **AnEAN**, **DMA-PEAN**, and **An$_2$*N*-PEAN** have orbital contribu-

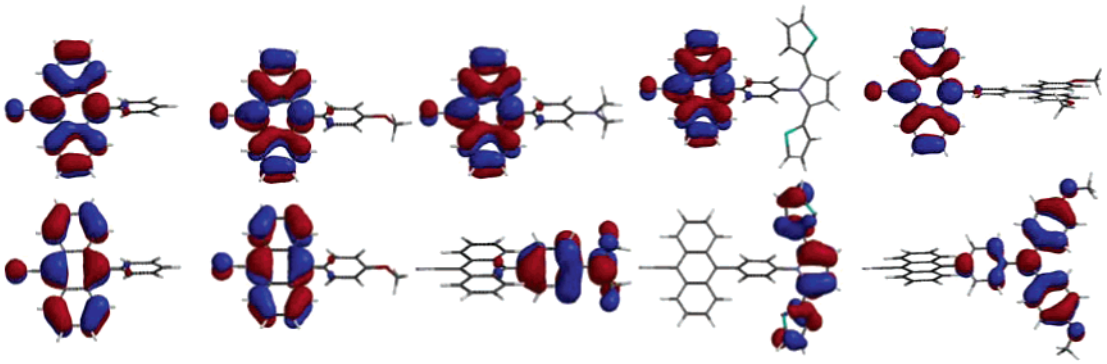

FIGURE 6. HOMO (bottom) and LUMO (top) orbital surfaces of (from left to right) **PAN**, **AnAN**, **DMA-PAN**, **DTP-PAN**, and **An$_2$*N*-PAN**.

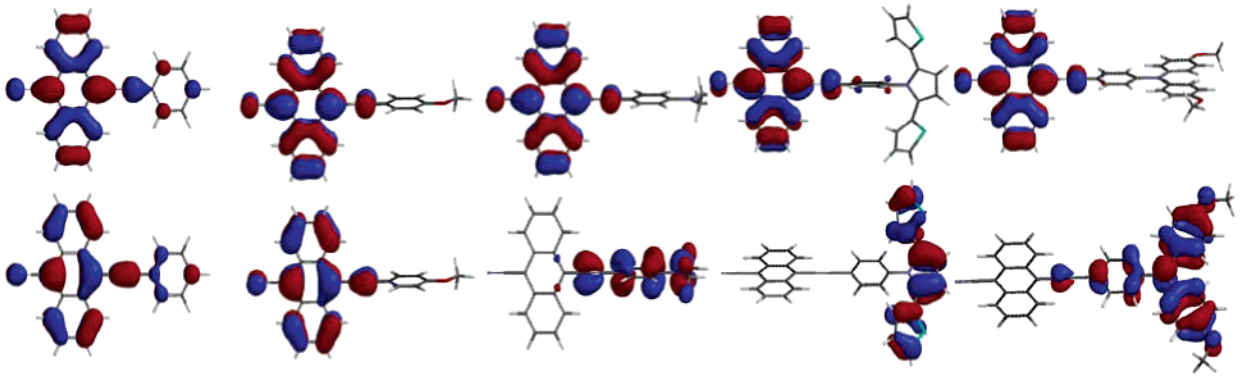

FIGURE 7. HOMO (bottom) and LUMO (top) orbital surfaces of (from left to right) **PEAN**, **AnEAN**, **DMA-PEAN**, **DTP-PEAN**, and **An$_2$*N*-PEAN**.

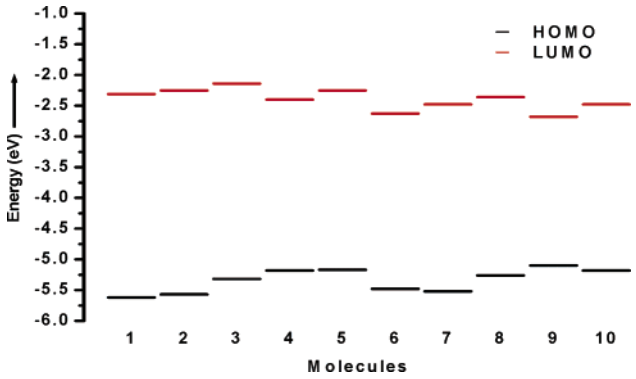

FIGURE 8. HOMO−LUMO energy levels of **PANs** and **PEANs**. Molecule code: **1**, **PAN**; **2**, **AnAN**; **3**, **DMA-PAN**; **4**, **DTP-PAN**; **5**, **An$_2$*N*-PAN**; **6**, **PEAN**; **7**, **AnEAN**; **8**, **DMA-PEAN**; **9**, **DTP-PEAN**; **10**, **An$_2$*N*-PEAN**. This energy level diagram shows the influence of the donor substituents on the HOMO and LUMO energies.

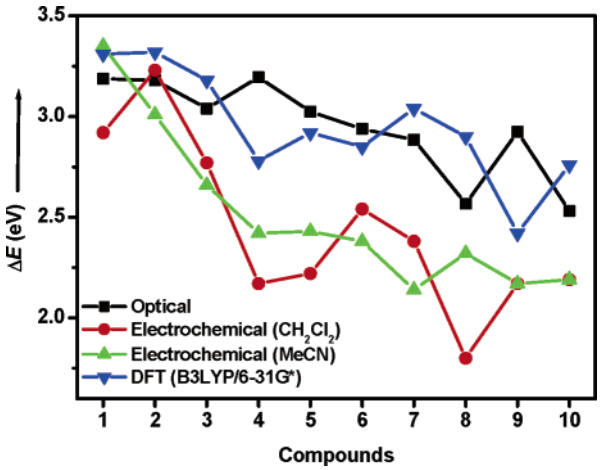

FIGURE 9. Comparison of experimental [optical (UV−vis λ_{max}/eV) and electrochemical] energy gaps with theoretical values. Compound code: **1**, **PAN**; **2**, **AnAN**; **3**, **DMA-PAN**; **4**, **DTP-PAN**; **5**, **An$_2$*N*-PAN**; **6**, **PEAN**; **7**, **AnEAN**; **8**, **DMA-PEAN**; **9**, **DTP-PEAN**; **10**, **An$_2$*N*-PEAN**.

tions similar to those of **PAN**, **AnAN**, **DMA-PAN**, and **An$_2$*N*-PEAN**, respectively. They additionally have contribution from the ethynyl linkage, and thus the ethyne participates in the electronic properties of these systems. The ethyne bridge does not seem to affect in any manner the properties of **DTP-PEAN**. The orbital coefficients of the latter indeed remain similar to that of **DTP-PAN**, despite the extension of π-conjugation by the C−C triple bond and hence the observed electronic properties.

The energy levels of HOMO and LUMO are of interest for study. As seen from Figure 8, both the HOMO energy and LUMO energy increase on increasing the strength of electron donors for the two series. However, the trend breaks at **DTP**-substituted **PAN** as well as **PEAN**, where the LUMO level is reduced when compared with the rest.

The energy gaps, values in electronvolts (eV), obtained from the theoretical calculations and UV−visible absorption maxima and electrochemical data, are depicted in the graph in Figure 9. Apart from a slight variation for each compound, there is a satisfactory correlation of the

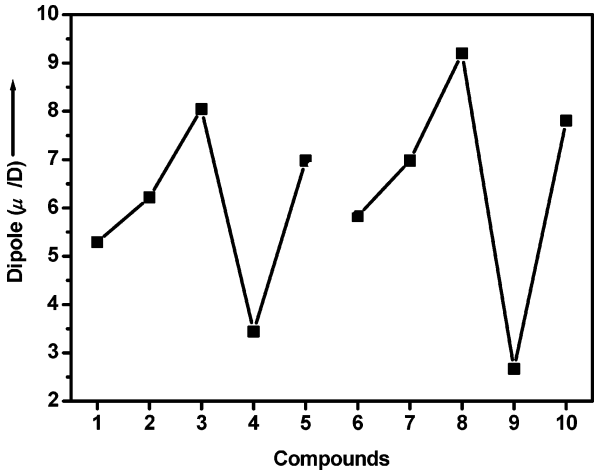

FIGURE 10. Calculated dipole moments of compounds. Compound code: **1**, **PAN**; **2**, **AnAN**; **3**, **DMA-PAN**; **4**, **DTP-PAN**; **5**, **An$_2$N-PAN**; **6**, **PEAN**; **7**, **AnEAN**; **8**, **DMA-PEAN**; **9**, **DTP-PEAN**; **10**, **An$_2$N-PEAN**.

data from theory and UV−vis absorption maxima in that all compounds show a similar trend except DTP-substituted molecules in **PAN** and **PEAN** series. While the observed electronic properties of all compounds can be well explained by the orbital coefficients obtained from the DFT calculations, the HOMO−LUMO gap as obtained from the DFT results and electrochemical results appears to differ vastly as with the DTP-substituted molecules (**DTP-PAN**, **4**, and **DTP-PEAN**, **9**), which also have wide difference in their energy gap values.

The intriguing electronic nature of the DTP-substituted systems is well augmented in the theoretical dipole moment, as shown in Figure 10. While the dipole increases upon increasing the electron donor strength, it reduces drastically in the case of DTP-substituted molecules in both **PAN** and **PEAN** series. The highest dipole among all compounds rests with the NMe_2-substituted molecules. The dipole vector always remains directed toward the cyanoanthryl subunit. Calculated dipole moments are in good agreement with the observed red shift in the emission maxima of the compounds. As the dipole moment increases from **PAN** to **DMA-PAN**, there is a gradual shift in the emission wavelength upon increasing the solvent polarity when going from **PAN** to **AnAN**. This applies to ethynyl counterparts as well (Figure 3). Again, as the dipole, as well as the emission maxima, of DTP-substituted molecules diminishes greatly in both **DTP-PAN** and **DTP-PEAN**, they do not vary with increasing solvent dielectric constant, indicating that these molecular dipoles do not interact with the medium and hence the observed spectra.

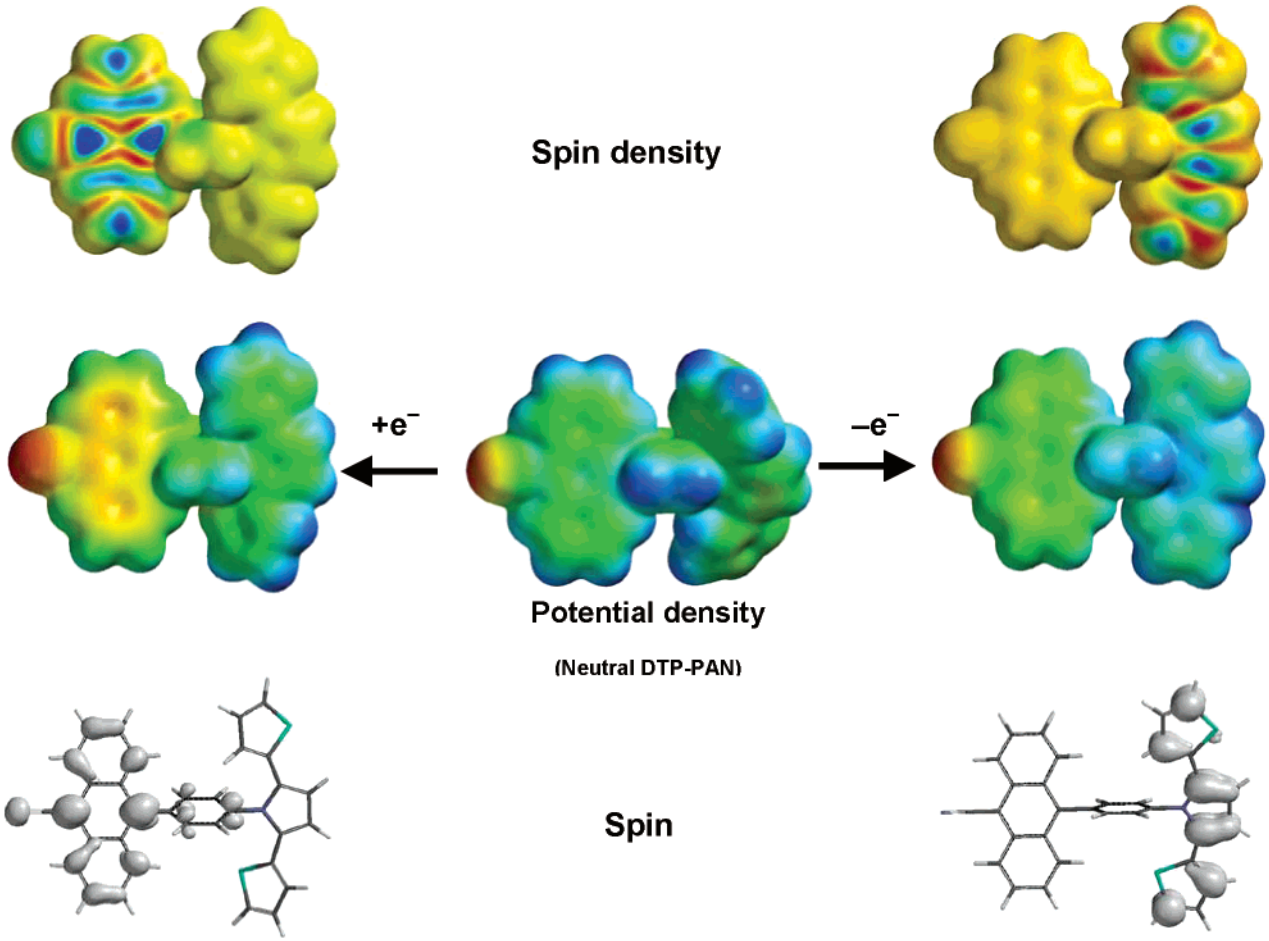

FIGURE 11. DFT-calculated changes in electrostatic potential surface, spin polarization, and spin density maps obtained after adding an electron to (one-electron reduction, left column) and removing an electron from (one-electron oxidation, right column) **DTP-PAN**.

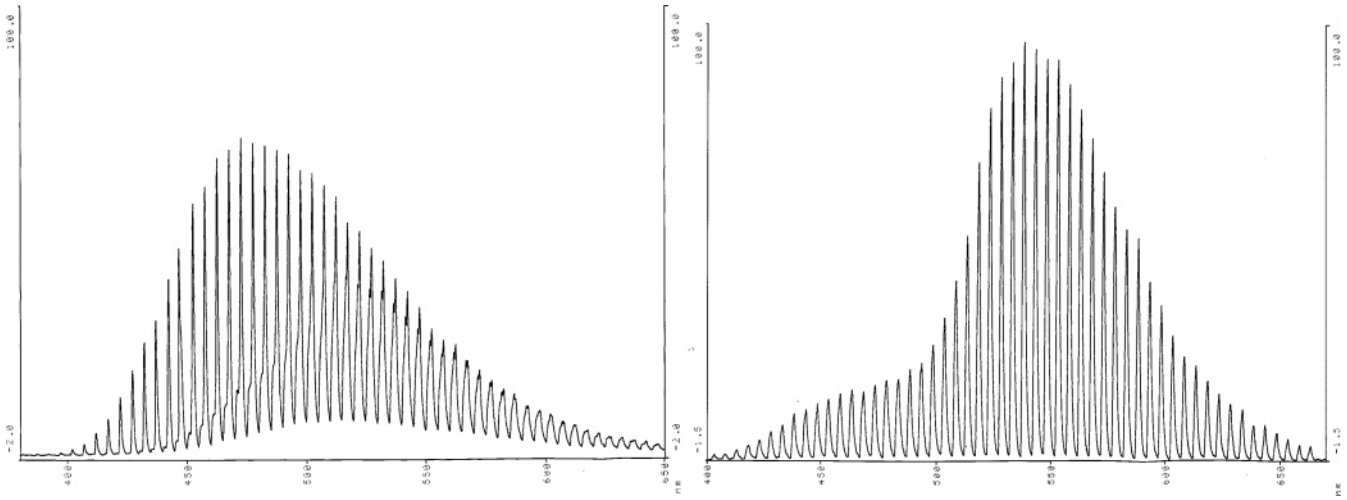

FIGURE 12. ECL spectra of **AnAN** (left) and **DMA-PAN** (right) recorded in CH_2Cl_2 (10^{-3} M) containing TBAP supporting electrolyte (50 mM).

It is of interest to us to investigate the nature of the charged molecules by DFT calculations in an attempt to gain maximum insight into their electronic structure. An expensive unrestricted HF model was to be incorporated for the optimization of the equilibrium geometry of these charged molecules. Figure 11 shows typical surfaces of one molecule, namely, **DTP-PAN**.

The potential density surface of the neutral molecules is shown at the center, and the spin density and spin surfaces are shown, respectively, on top and bottom. The structures on the left column represent the result of one-electron reduction, and those on the right represent the outcome of one-electron oxidation. As evident in Figure 11, the reduction process adds an electron to the molecule, and as a result of the strong electron-withdrawing nature of the acceptor AN moiety, the electron reaches this part of the molecules and resides on it. The electrostatic potential shows more (red) negative density at this part. The spin density, as well as the spin surface on the left-hand side, depicts clearly the existence of the added electron at the acceptor moiety **AN**. On the other hand, removal of an electron from the neutral molecules produces an oxidized species, and the positive charge (the radical cation) resides at the donor part showing the oxidation occurring on this moiety. The donor moiety attains lass electron density (more blue), and the corresponding spin density map and the spin surface further confirm this observation. As a result of removal of an electron, the donor and acceptor moieties attain coplanarity, but the bridge phenylene remains uninvolved and twisted.

The ethyne counterpart of the above molecule, **DTP-PEAN**, showed a slightly different trend as the charging produced species in which the phenylene unit, which retained a 63.39° dihedral angle with the acceptor in its neutral form, attains coplanarity with the acceptor **AN** moiety upon receiving an electron.[20] Thus, the spin polarization can be achieved by using this kind of donor and acceptor to produce molecules suitable for electronic applications.

Electrochemiluminescence. ECL spectra were recorded in acetonitrile at 1.0 and 0.10 mM concentrations with 50 mM tetrabutylammonium perchlorate as a supporting electrolyte in a cell setup similar to the previously published one.[21] The electrodes were pulsed between first oxidation and first reduction peak potentials at various pulse intervals in order to generate radical ions and induce annihilation reaction. Satisfactory ECL spectra were obtained at a 10^{-3} M concentration of sample solution, while no ECL was observed at lower or higher concentrations.

The ECL maxima (Table 2) for **PAN**, **AnAN**, **DMA-PAN**, and **DMA-PEAN** are very close to the photoluminescence maxima recorded in Table 1. They can be considered as emitting from their monomeric S^1 state ($-\Delta H$ values higher than ECL emission maximum in eV). All other molecules in both the **PEAN** and **PAN** series show ECL emission red-shifted by >80 nm, and they have energy insufficient to populate the singlet state; thus, they followed the T-route (triplet−triplet annihilation) to produce the emitting state.

The appearance of the ECL spectra of **AnAN** and **DMA-PAN** is interesting (Figure 12). Even though **AnAN** displays predominantly monomer ECL, there is a latent tendency for this molecule to produce the excimer state as seen from an inherent poorly generated shoulder around 525 nm that exists within the monomer emission band. **DMA-PAN** shows a shoulder at a higher energy area of the spectrum, indicating the tendency for formation of a blue-shifted ECL. Full formation of blue-shifted ECL with respect to photoluminescence spectra of structurally related compounds have been well studied and documented from our labs.[22]

Conclusion

Conjugated donor−acceptor molecules based on 9-cyanoanthracene have been prepared by Suzuki coupling

(20) Optimization of radical cation failed after 3 days, 25 iterations.

(21) (a) Chen, F.-C.; Ho, J.-H.; Chen, C.-Y.; Su, Y. O.; Ho, T.-I. *J. Electroanal. Chem.* **2001**, *499*, 17. (b) Elangovan, A.; Chen, T.-Y.; Chen, C.-Y.; Ho, T.-I. *Chem. Commun*. **2003**, 2146.

(22) (a) Elangovan, A.; Yang, S.-W.; Lin, J.-H.; Kao, K.-M.; Ho, T.-I. *Org. Biomol. Chem.* **2004**, *2*, 1597. (b) Elangovan, A.; Chiu, H.-H.; Yang, S.-W.; Ho, T.-I. *Org. Biomol. Chem*. **2004**, *2*, 3113. (c) Ho, T.-I.; Elangovan, A.; Hsu, H.-Y.; Yang, S.-W. *J. Phys. Chem. B* **2005**, *109*, 8626. (d) Elangovan, A.; Lin, J.-H.; Yang, S.-W.; Hsu, H.-Y.; Ho, T.-I. *J. Org. Chem*. **2004**, *69*, 8086. (e) Elangovan, A.; Kao, K.-M.; Yang, S.-W.; Chen, Y.-L.; Ho, T.-I.; Su, O. Y. *J. Org. Chem*. **2005**, *70*, 4460.

and Sonogashira coupling approaches in order to get directly linked and enthyne-bridged bipolar centers. All 10 compounds show interesting electronic characteristics. While directly linked Suzuki coupling products show absorption properties comparable with free AN, their ethyne-bridged counterparts possess more favorable properties in that the electronic absorption and fluorescence emission maxima are very much shifted to the longer wavelength regions. *N*,*N*-Dimethylaminophenylanthronitrile (**DMA-PAN**)[17] provides a guideline for the interpretation of the observed photophysical properties of the whole set of molecules. As stated,[17a,h] this molecule exhibits TICT in medium-polarity solvents such as benzene, methylene chloride, and THF, while it shows normal LE emission in other solvents. Similar behavior is observed in the case of triarylamino donor-bearing anthronitrile, **An$_2$*N*-PAN**, but not in dithienylpyrrole-bearing phenylanthronitrile, **DTP-PAN**. There appears to be no electronic communication between the DTP donor and AN acceptor. The ethynes on the other hand exhibit no TICT character in either the triarylamino donor system or the DMA donor system. The adherence of selected molecular systems to the Lippert equation explains the molecular environment dependence of the Stokes shift. Very good correlation has been made for the true ICT molecule, but poor correlation was noticed for poor- or non-ICT systems.

The electrochemical behavior has been well documented and was found to be affected by the introduction of both variable donor strengths and an ethyne bridge. All but one molecule show ECL emission; those showing monomer ECL do so from the singlet state, while those exhibiting excimer ECL do so via the triplet−triplet annihilation route as explained by the difference in the ECL emission energy and annihilation enthalpy change.

Density functional theory has been found to provide support for the observed electronic properties of the systems studied in this work. Extensive open-shell calculations for all molecules require expensive computational power, though we have been able to provide the results of open-shell calculations for the DTP-based system, while closed-shell calculations for all molecules offer excellent correlation with the observed electronic properties. The power and use of quantum chemical calculations have been well established. The present study offers opportunity for further development of novel functional organic materials for electronic applications in addition to providing a basic understanding of the mechanisms governing the electron-transfer processes in π-conjugated donor−acceptor arrays.

Acknowledgment. Financial support for this work was provided by the National Science Council, Taiwan.

Supporting Information Available: Complete ref 8a, general experimental methods, characterization data, ^{1}H NMR, ^{13}C NMR, multiscan CV and raw ECL, spectra all compounds, Cartesian coordinates for all neutral molecules and radical ions of **DTP-PAN** and **DTP-PEAN**, and solvatochromic data tables (XLS). This material is available free of charge via the Internet at http://pubs.acs.org.

JO051183G